

Fragment Formation in Central Heavy Ion Collisions at Relativistic Energies

E. Santini, T. Gaitanos, M. Colonna, M. Di Toro¹

*Laboratori Nazionali del Sud INFN, Physics and Astronomy Department,
University of Catania, I-95123 Catania, Italy*

Abstract

We perform a systematic study of the fragmentation path of excited nuclear matter in central heavy ion collisions at the intermediate energy of 0.4 AGeV. The theoretical calculations are based on a Relativistic Boltzmann-Uehling-Uhlenbeck (*RBUU*) transport equation including stochastic effects. A Relativistic Mean Field (*RMF*) approach is used, based on a non-linear Lagrangian, with coupling constants tuned to reproduce the high density results of calculations with correlations.

At variance with the case at Fermi energies, a new fast clusterization mechanism is revealed in the early compression stage of the reaction dynamics. Fragments appear directly produced from phase-space fluctuations due to two-body correlations. In-medium effects of the elastic nucleon-nucleon cross sections on the fragmentation dynamics are particularly discussed. The subsequent evolution of the primordial clusters is treated using a simple phenomenological phase space coalescence algorithm.

The reliability of the approach, formation and recognition, is investigated in detail by comparing fragment momentum space distributions *and simultaneously* their yields with recent experimental data of the *F0PI* collaboration by varying the system size of the colliding system, i.e. its compressional energy (pressure, radial flow). We find an excellent agreement between theory and experiment in almost all the cases and, on the other hand, some limitations of the simple coalescence model. Furthermore, the temporal evolution of the fragment structure is explored with a clear evidence of an earlier formation of the heavier clusters, that will appear as interesting *relics* of the high density phase of the nuclear Equation of State (*EoS*).

Key words: Heavy ion collisions at intermediate energies, Fragment formation, Rapidity distributions, Nuclear matter, Equation of state, In-medium cross sections, Dirac-Brueckner-Hartree-Fock

PACS: 25.75.-q, 25.75.Ld, 21.65.+f

¹ ditoro@lns.infn.it

1 Introduction

One of the major interests in the study of intermediate energy ($0.1 - 1$ AGeV) Heavy Ion Collisions (*HIC*) is the determination of the nuclear matter Equation of State (*EoS*) under conditions of density and/or temperature beyond saturation. During the last two decades many attempts have been successfully done in this direction, see Refs. [1] for an overview. It turned out that baryon collective flow strongly depends on the high density behavior of the nuclear *EoS*. Experimental studies on collective flow have suggested a rather “soft” *EoS* at supra-normal densities [2] which has a similar functional dependence as that obtained from microscopic Dirac-Brueckner-Hartree-Fock (*DBHF*) theory [3]. Also particle production, in particular subthreshold Kaon (K^+) yields are affected by compressional effects of the high density region. Experiments on particle production have strongly supported a “soft” *EoS* at high densities [4,5].

However, one has to realize that a *HIC* is a rather complicated non-equilibrium process. A unique determination of the nuclear *EoS* far away from saturation requires a complete characterization of the collision dynamics in comparison with experimental data when available. It has been experimentally shown that the final state of a *HIC* at intermediate energies is dominated by fragments with a strong collective flow pattern relative to that of free protons. In particular, more of 70% of protons are bound to clusters [6]. The collective baryon flow is thereby connected to that of the fragment flow in terms of a linear dependence with respect to the fragment charge [7,8]. It therefore turns out that the description of the process of fragmentation is very important in theoretical transport studies of an entire characterization of the reaction dynamics (apart the dynamical behavior of nucleons and produced particles).

Here we will concentrate on the fragment production in central *HIC* at intermediate energies. This study is particularly interesting since it could be compared to the clusterization mechanism evidenced at lower energies, based on a growth of spinodal instabilities leading to a Liquid-Gas (*LG*) phase transition [9]. The latter mechanism is active in the expansion phase of the excited nuclear system during the reaction dynamics and so it gives information on the low density behavior of the nuclear *EoS*. It is important to note that similar signatures have been found in peripheral fragmentation at higher energies [10], where actually the first evidence of a nuclear *LG* phase transition was revealed.

Both scenarios, central collisions at the Fermi energies and projectile fragmentation at intermediate energies, have in common the presence of a fragmenting source without a large radial flow, i.e. a relatively low expansion velocity [10,11]. In central collisions in the $(0.1 - 1)$ AGeV range we have a much faster

expansion of the interacting nuclear matter and the spinodal mechanism will be largely hindered due to the mismatch between the timescales of the instability growth and of the expansion. The picture appears even worse for a low-density nucleation mechanism. In fact in this case we have a non-vanishing surface tension leading to a barrier which needs to be overcome, with a further increase of the relevant time-scale.

Clusters are then expected to come directly from correlations in the high density region, actually partially reduced during the expansion. Consistently the size distribution will be very different, much more dominated by light ions, since the characteristic wavelengths of the mean field instabilities [9] will not play any role. If this picture is correct, we will have a chance to see in the fragment properties some direct effects of the nuclear *EoS* at high density. This will be particularly valid for the heavier fragments, that could be considered as the *relics* of the high density phase.

The microscopic transport models have proven to be an adequate tool for the description of the non-equilibrium reaction dynamics at intermediate energies [12–15] (see for recent results [16]). The physical input of such semi-classical models based on Boltzmann type equations are the nuclear mean field and the nucleon-nucleon cross sections. Both can be derived either directly from the effective two-body in-medium interaction, i.e. the in-medium G-matrix [17] or phenomenologically from Skyrme- and Walecka-type models [18,19]. Although Boltzmann type transport models describe the dynamics of the single-particle distribution function very satisfactory, they do not provide information on the dynamical evolution of (physical) fluctuations which are important in understanding the fragmentation mechanism. Different ways have been proposed to include the evolution of higher order correlations beyond the mean field level: by adding a fluctuation term (Boltzmann-Langevin equation) [20], by choosing the numerical fluctuations in a judicious way just by limiting the number of test particles [21], or finally by introducing fluctuations directly into the single-particle phase space distribution function [22,23]. The detailed consequences of these different approaches are still under intense investigation. Here we will follow the second procedure, numerically easy to implement in the transport code, based on the noise of a discrete mapping of the phase space. This approach allows to maintain in the dynamics the random effects of the collision term, that otherwise would be completely washed out in presence of a large number of test-particles [24]. Thus, the collision term will be able to initiate fluctuations leading to a cluster formation, as suggested in ref. [25]. This description looks particularly suitable in the present case for clusters produced on a very short time scale in the compression phase. Such high density clusterization mechanism has been suggested also in other non-relativistic dynamical transport models, like Quantum Molecular Dynamics (*QMD*) [26,13,27] and Boltzmann-Uehling-Uhlenbeck (*BUU*) [28] approaches. Here we investigate in detail the fragment dynamics, yields and velocity distributions, and the

dependence on the size of the colliding systems.

The fragment recognition in the *HIC* dynamics consists of a phenomenological procedure, the phase-space coalescence model [29], which has been successfully implemented within mean field transport simulations in the past [14,18,30]. Its advantage is that it can be easily applied to the final phase space distribution function, in order to realistically compare with experiments which require information on fragment yields. The determination of the final state of a *HIC* in terms of baryons *and* fragments is furthermore necessary in theoretical simulations in order to use the same methods as in the experiments to characterize the events, i.e. reaction plane resolutions, centrality selections using charge particle multiplicities or other related observables. Here we extend its use even to provide information on how the system develops through after the initial cluster formation.

The idea of the present work is to investigate the reliability of this fragmentation path, formation and further evolution, in intermediate energy heavy ion collisions, taking the chance of the existence of new experimental data from the *FOPI* collaboration [31,32]. To do so, we first describe the main ingredients of the stochastic transport model and the phase space coalescence algorithm, and then apply them to *HIC* reaction dynamics and compare the theoretical results with all available experimental data related to fragment production. In particular, the system size dependence of fragment velocity distributions and yields is investigated in detail.

2 Fragment description in RBUU

The traditional approach to theoretically investigate heavy ion collisions is the transport equation of a Boltzmann type, called as Relativistic-Boltzmann-Uhlenbeck-Uheling (*RBUU*) equation, which is described in detail in refs. [17–19]. The *RBUU* equation has the form

$$\left(k_\mu^* \partial_x^\mu + (k^{\nu*} F^{\mu\nu} + m^* (\partial^\mu m^*)) \partial_\nu^{k^*} \right) f(x, k^*) = \frac{1}{2} \frac{1}{(2\pi)^3} \int \frac{d^3 k_1^*}{k_1^{*0}} \frac{d^3 k_1^{*'}}{k_1^{*0'}} \frac{d^3 k_1^{*'}}{k_1^{*0'}} \times W(k^* k_1^* | k_1^{*'} k_1^{*'}) \left[f(x, k^{*'}) f(x, k_1^{*'}) (1 - f(x, k^*)) (1 - f(x, k_1^*)) - f(x, k^*) f(x, k_1^*) (1 - f(x, k^{*'})) (1 - f(x, k_1^{*'})) \right] \quad (1)$$

Eq. (1) describes the evolution of the single particle distribution function $f(x, k^*)$ under the influence of a mean field, which enters via effective masses m^* , effective momenta k^* and the field tensor $F_{\mu\nu}$, and of binary collisions.

The numerical solution of the *RBUU* equation is based on the test particle method using Gaussian functions (first introduced in Ref. [33]), in which each nucleon is represented by a finite sum of test particles. In fact one uses covariant Gaussian's (in Minkowski and momentum space) adopting the Relativistic Landau-Vlasov (*RLV*) method [34]. In [11] it was shown that the *RLV* method is appropriate to produce smooth fields and it is possible to determine local quantities, such as densities, local momentum distributions, etc., without introducing additional grids. The collision integral includes all inelastic channels up to pion production. The energy and angular dependence of the inelastic cross sections are taken from Ref. [35]. For the elastic cross sections we will use two options: (a) the free parametrizations according Cugnon et al. [36] and (b) the in-medium effective cross sections from the Tuebingen-group [37].

Within the Relativistic Mean Field (*RMF*) frame a non-linear Lagrangian is used, which leads to a soft *EoS* at high densities, similar to that derived from correlated Dirac-Brueckner-Hartree-Fock *DBHF* approaches [38,39]. In this way one is able to reproduce the single-particle dynamics very satisfactory in terms of collective flow observables of nucleons and other produced particles as outlined in the introduction [38,39]. In the isovector channel scalar and vector field contributions are included, with coupling constants also derived from *DBHF* estimations [38,39]. Moreover, a comparison with experiments requires in any case the knowledge of the degree of clusterization, in order to perform the flow analysis in the same way as in the experiment [7,8].

According to the phase space coalescence procedure, a number of nucleons can form a cluster if their distances in coordinate and momentum space are smaller than a given set of coalescence parameters R_c , P_c , respectively. These parameters can be fitted by adjusting the charge distributions, as it has been already shown in Refs. [30]. However, so far more detailed dynamical properties of fragments, recognized by means of a phase space coalescence, have not yet been studied due to the missing of precise experimental information.

Very recently the *F0PI* collaboration has performed a systematic analysis on fragment velocity distributions and yields in terms of rapidities in beam and in transverse (with respect to the beam axis) directions [31,32]. The experimental analysis has also been extended to study the system size dependence of the degree of clusterization and fragment flows. Thus, by fitting the coalescence parameters just on global charge distributions one is now able to test in detail the phase space coalescence model on more exclusive observables of the reaction dynamics in an essentially parameter-free way.

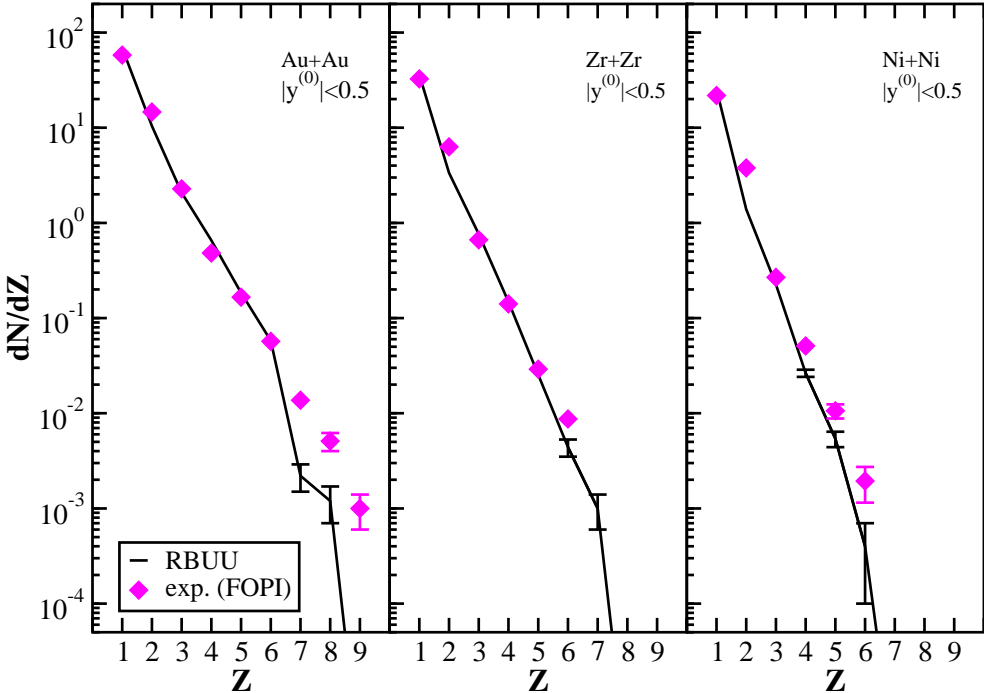


Fig. 1. Charge distributions at mid rapidity ($|y^0| < 0.5$, [42]) for central ($b^{(0)} \leq 0.15$, [43]) collisions for different systems (as indicated) at 0.4 AGeV incident energy. The theoretical curves (solid lines) performed within the *RBUU* transport model are compared with experimental data (diamonds) from the *F0PI* collaboration [31].

3 Application to heavy ion collisions

We have performed simulations of heavy ion collisions at an intermediate incident energy per nucleon of 0.4 AGeV using the *RBUU* equation for the evolution of the phase space distribution function and the phase space coalescence applied in the final state of each *RBUU* event. Clusters are identified at a *freeze – out* time of $90 \text{ fm}/c$, when they are well separated in phase space. As shown later, when we will look at the time evolution of the cluster structures, these “final” results are not much depending on the choice of the *freeze – out* time, which is obviously varying with the beam energy. This is important in order to get information on system size effects at a given beam energy.

In fact, in order to compare with the available data, the analysis has been performed by varying the system size, from (Ca, Ca) to (Au, Au) reactions, and focussing on central collisions. Experimentally the observable *ERAT* has been adopted to select the most central events. Theoretically we use the same observable (see Ref. [15]) with the result of a centrality resolution consistent with the experimental one. One should note that similar studies adopting the Isospin-Quantum-Molecular-Dynamics (*IQMD*) model predict the same impact parameter selections [8]. All the results discussed in the following have been obtained with a soft *EoS* (at supra-normal densities) with a compression

modulus of 200 MeV and using *free* and *effective* NN cross sections. In order to obtain a reasonable statistics for cluster studies, we have performed a coalescence procedure to 5000 random samplings of A nucleons for each “stochastic” $RBUU$ event, for given initial condition. As discussed before one “stochastic” $RBUU$ event corresponds to a transport calculation with about 50 test particles (phase space gaussians) per nucleon. This number is in fact varying with the size of the system in order to have the same global phase-space mapping when we change the number of nucleons, a *total* number of test particles around 15000. We have checked that this mapping ensures a good time evolution of mean one-body observables allowing the development of local fluctuations from direct nucleon-nucleon interactions.

3.1 Charge particle distributions

Fig. 1 shows the charge particle distributions at mid rapidity for three different colliding systems ($Au + Au$, $Zr + Zr$ and $Ni + Ni$ at 0.4 $AGeV$ incident energy). It can be seen that the theoretical results fit the experimental data very well. The extracted coalescence parameters have been chosen as $4.5\ fm$ and $1.5\ 1/fm$ in coordinate and momentum space, respectively. One should note that these parameters, once fixed from the $Au + Au$ charge distribution, are unique for all the systems considered here.

In fact these estimations represent some “effective” coalescence parameters, partially related to the amount of fluctuations inserted in the $RBUU$ simulations via the discrete test-particle mapping of phase-space. Indeed from the sampling procedure described before we can expect that if we increase the total number of test-particles we can reduce the coalescence parameters. As already noted we have to find a compromise with the need of a limited number of test-particles that will allow the development of local fluctuations. We have checked the stability of the results vs. a factor two change of the total number of test-particles given before. It is essential to keep the coalescence parameters fixed for all studied colliding systems, we can then trust the reliability of the physics results.

The moderate discrepancies between theory and experiment for the heavier clusters ($Z > 5 - 6$), reported in Fig. 1, will not influence most of the results shown below, due to their low multiplicity with respect to that of protons and light ions. We will see later that in fact these heavier fragments are associated to a very interesting physics and so the lack of statistics, in simulations as well as in experiments, represents a serious drawback.

We note how well the simulations are reproducing the increasing slope of the $N(Z)$ exponential behavior with decreasing system size. This doesn’t mean

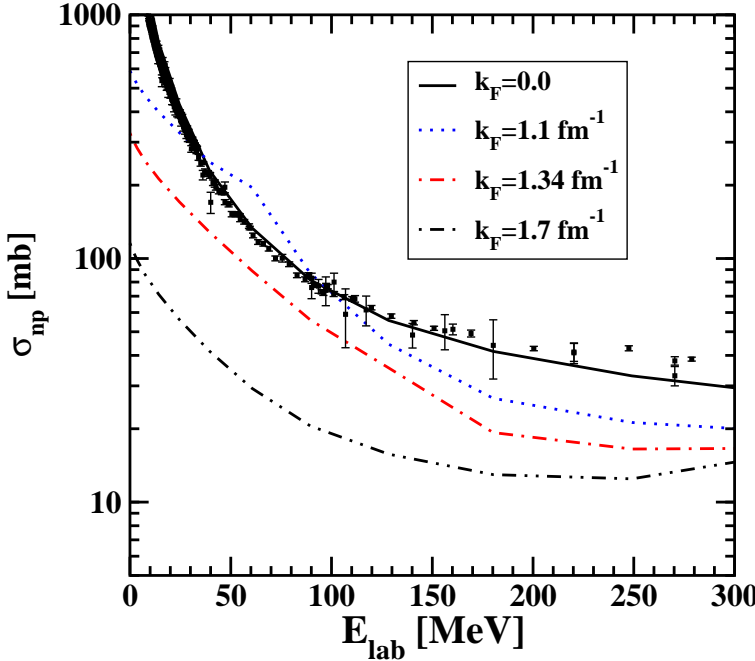


Fig. 2. Elastic in-medium neutron-proton cross sections at various Fermi momenta k_F as function of the laboratory energy E_{lab} . The free cross section ($k_F = 0$) is compared to the experimental total np cross section [40] (crosses).

that lighter systems become “hotter” but just that we have less stopping while the fragments, in particular the heavier ones, are produced in the dense phase. This “non-equilibrium” interpretation will be clear in the following and in fact it has been already suggested from the analysis of experimental data in ref. [31].

In connection to the previous point, with the fixed coalescence parameters one can now start to study the reaction dynamics in terms of the degree of transparency and related variances, i.e. in terms of the rapidity distributions of fragments along the beam and transverse directions.

In central collisions at intermediate energies the degree of stopping is mainly influenced by the binary collisions or the viscous behavior of the system. More (less) collisions lead to less (more) viscosity, i.e. more (less) local equilibration and thus to less (more) transparency of the colliding matter. The connection between the reaction dynamics and the viscous behavior has been studied in Ref. [32,41]. It was shown that in-medium effects of the elastic nucleon-nucleon (NN) cross sections are important for a reliable description of the reaction dynamics as far as the baryon stopping and flow is concerned. It is therefore of great interest to see whether in-medium effects of the NN cross section influence the fragment dynamics. We will study first this important topic in the following subsection.

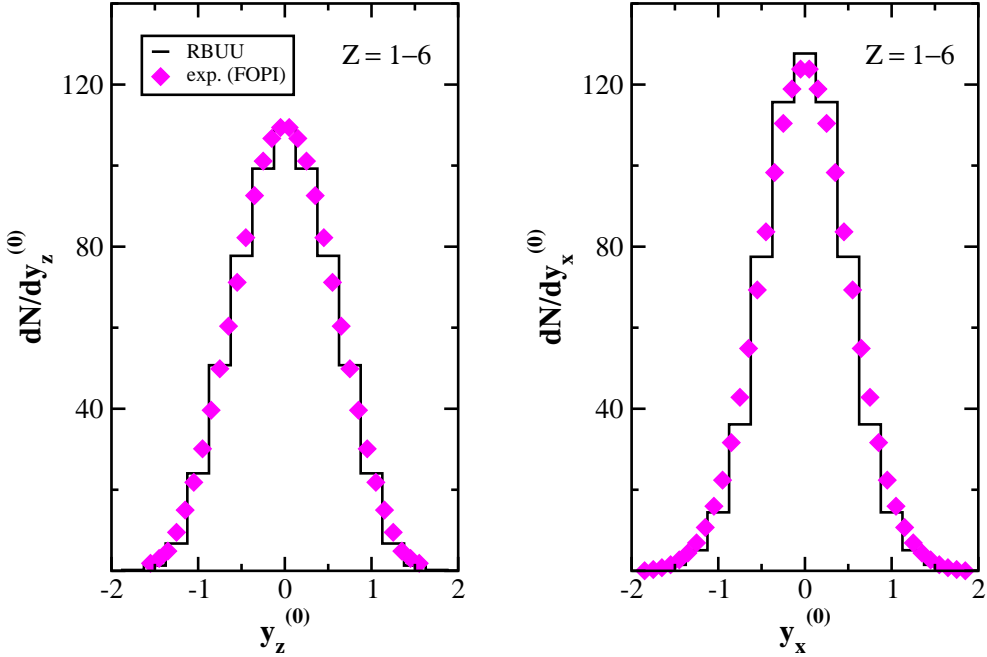


Fig. 3. Longitudinal (left) and transversal (right) rapidity distributions [42] for all charged ions up to $Z = 6$ (weighted with their charge) for central ($b^{(0)} \leq 0.15$) $Au + Au$ collisions at 0.4 $AGeV$ incident energy. Theoretical *RBUU* calculations (solid histograms) are compared with *FOPI* data (diamonds) from [32].

3.2 In-Medium effects of the elastic NN cross sections on clusters

Fig. 2 shows the energy dependence of the in-medium neutron-proton (np) cross section [37] at Fermi momenta $k_F = 0.0, 1.1, 1.34, 1.7 fm^{-1}$, corresponding to the densities $\rho \sim 0, 0.5, 1, 2\rho_0$ ($\rho_0 = 0.16 fm^{-3}$ is the nuclear matter saturation density). The presence of the medium leads to a substantial suppression of the cross section which is most pronounced at low laboratory energy E_{lab} and high densities where, in addition to the $(m^*/m)^2$ scaling, the Pauli-blocking of intermediate states is most efficient [37]. At larger E_{lab} asymptotic values of 15–20 mb are reached. However, not only the total cross sections but also the angular distributions are affected by the presence of the medium. The initially highly forward-backward peaked (n, p) cross sections becomes much more isotropic at finite densities [37] which is mainly due to the Pauli suppression of soft modes (π -exchange) and corresponding higher partial waves in the T-matrix. In Ref. [41] it was shown that the reduced effective cross sections considerably influence the degree of transparency and improves the comparison with the data. This is illustrated in Fig. 3 for the $Au + Au$ case, where the longitudinal and transversal rapidity distributions of all charged particles (weighted with their charge) are displayed. The theoretical calculations using the effective cross sections reproduce the experimental data very well. Not only the longitudinal, but also the transversal rapidity distribution compares well with the experimental data. The same conclusion is valid even for other

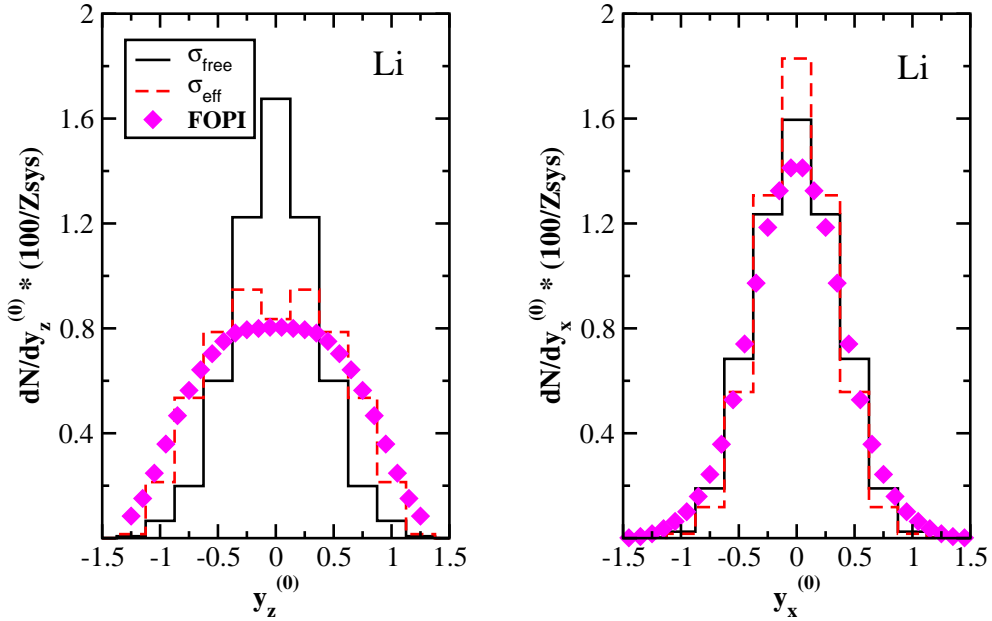


Fig. 4. Scaled longitudinal (left) and transversal (right) rapidity distributions for Li -fragments for central ($b^{(0)} \leq 0.15$) $Ru + Ru$ collisions at $0.4 AGeV$ incident energy. Theoretical calculations using free and in-medium NN cross sections (solid and dashed histograms, respectively) are compared with $FOPI$ data (diamonds, from [31]). The ordinates are normalized to a constant system size of $Z = 100$ nuclear charge, as in ref. [31].

incident energies, for details see Ref. [41].

Obviously the question appears if the fragment dynamics is affected by density effects on the NN cross sections. The in-medium effects of the microscopic NN cross sections influence the stopping features not only of the protons but particularly those of the fragments, as shown in Fig. 4 for the $Ru + Ru$ case. Here the longitudinal and transverse rapidity distributions of $Z = 3$ clusters obtained from transport calculations using free and the effective NN cross sections are compared with each other and with recent data. It is shown that the transparency effect is more pronounced with the (reduced) in-medium NN cross sections and the distributions fit better with the experiment in this case.

This observation, which is similar to that of protons, is a non-trivial feature. The in-medium effects on the cross sections become important at higher densities due to the influence of the (intermediate state) Pauli operator and the reduction of the effective mass. Thus this result clearly indicates that fragments are formed earlier, during the stage where the local densities are still high, then one can obviously expect in-medium effects on the stopping power of fragments, and also on the yields (total areas in Fig.4). In any case it turns out that the use of in-medium effects within a consistent basis (mean field and collision integral) is crucial in describing the reaction dynamics of central col-

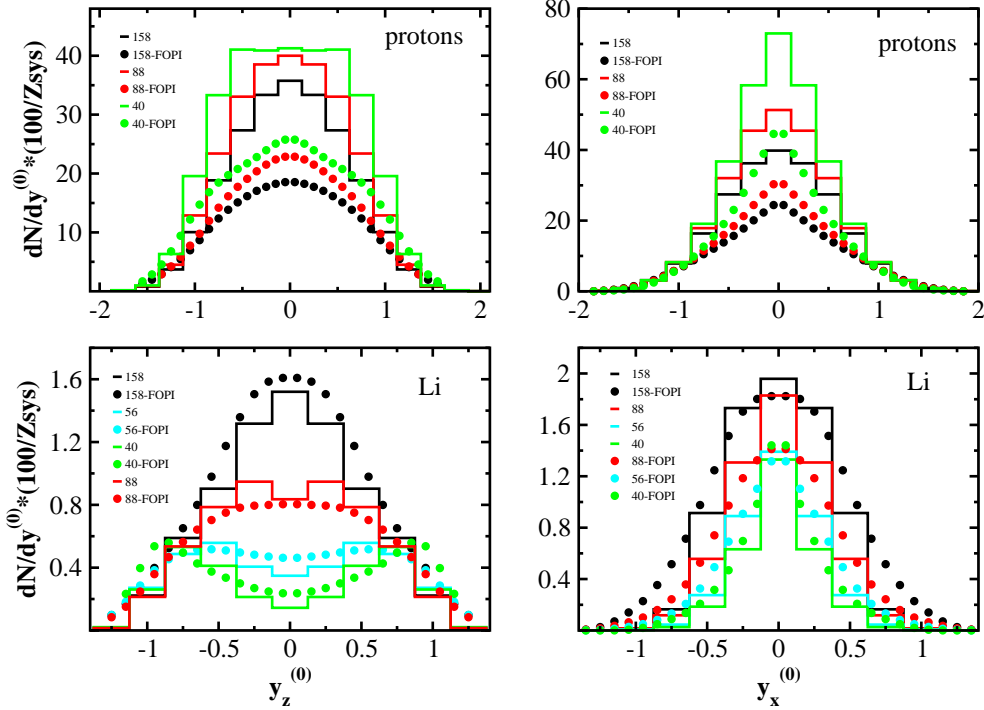


Fig. 5. Scaled longitudinal (left) and transversal (right) rapidity distributions of single protons (top) and Li clusters (bottom) in central ($b^{(0)} \leq 0.15$) collisions at 0.4 $AGeV$ incident energy for different symmetric systems. The various system charges Z_{sys} are indicated in the figure. The ordinates are normalized to a common reference system with charge $Z_{sys} = 100$. Theoretical calculations (histograms) are compared with *FOPI* data (symbols) from [31].

lisions. In conclusion all the simulation results shown here have been obtained using the in-medium parametrizations of the NN cross sections discussed before, with the related energy, density and angular dependences [37].

3.3 Transparency features of protons and clusters

Fig. 5 shows the longitudinal (dN/dy_z) and transversal (dN/dy_x) rapidity distributions of free protons (top) and light clusters (bottom) for central collisions for different colliding systems, as indicated. The centrality classes ($b^{(0)} \leq 0.15$) has been extracted in the same way as in the experiment [31]. In general we observe a degree of transparency since the longitudinal rapidity distributions are in all cases broader compared to the transverse ones. However the size dependence of the transparency effect is indicatively different for protons vs fragments, see the left panels of Fig. 5. For ($Z = 3$) ions it increases as the system size decreases: for the lightest system ($Ca + Ca$) the fragments are mainly formed in the spectator regions, lower-left panel of Fig. 5. The transparency effect of protons shows just the opposite trend. These results, in nice agreement with the data, further support the interpretation of an important dynamical cluster formation at higher densities. For light systems we cannot build high

densities at mid-rapidity and we observe a sharp drop in the fragment yield to the advantage of a proton emission. In conclusion the internal composition of the source is different for participant ($|y_z^{(0)}| < 0.5$) and spectator ($|y_z^{(0)}| \sim 1$) matter with respect to the system size of the colliding system. The heavier system exhibits a stronger “liquefaction” whereas by decreasing the size one observes an essential reduction of clusterization of the mid rapidity source. Only close to the spectator regions one sees an “universality” behavior independent of the system size (apart the lightest *Ca*-system) exactly like in the data. This universality behavior should not be confused with similar findings of the *ALADIN* collaboration where peripheral collisions were studied with a clear separation of spectator fragmentation [44], see the detailed discussion in ref.[31].

The transverse rapidity distributions, right panels of Fig. 5, appear also very instructive. As in the data, the proton yields for heavier systems are dropping in the smaller $|y_x^{(0)}| < 0.7$ transverse rapidities, where more clusters are formed. The widths of the cluster distributions are systematically increasing with the size, in the simulations as well as in the data. In a statistical picture this could indicate an increase of the source temperature with the size, at variance with the indications of the charge particle distributions, see the comments after Fig.1. In a dynamical interpretation of the fragment production the apparent contradiction disappears. The reduced stopping of the lighter systems, responsible of the faster decrease of the $N(Z)$ curves in Fig.1, will also imply reduced fluctuations in the nucleon phase space distributions. Moreover, we will have even a reduced radial flow that is decreasing the transverse velocity widths, as stressed in ref.[31]. In conclusion fragments are more formed if matter is more stopped. This evidence is further supporting the “high-density” origin. In fact at the Fermi energies we observe just the opposite: the multiplicity of fragments, produced now in the low-density phase, is decreasing when increasing the NN cross sections [45].

A difficulty appears in the absolute values of the (free) proton yields, upper panels of Fig.5. On the other hand, our estimations were appropriate for the multiplicities of $Z = 1$ ions, Fig.1 and the (weighted) rapidity distributions for $Z = 1 - 6$ charges, Fig.3. A possible explanation could be the failure of the present naive phase space coalescence model in describing the deuteron multiplicities. One can think that the description of all the fragments with the same set of coalescence parameters would not be appropriate for deuterons due to their relatively large *rms* radius ($r_d = 1.96$ fm [46], e.g. compared to the radius of *t* and *He* fragments, $r_{t,He} = 1.61, 1.74$ fm [47], respectively). In fact, we obtain more free protons relative to deuterons. This explains the fact that the $Z = 1$ multiplicity (which does not distinguish between protons and $Z = 1$ fragments) can be well reproduced, in contrast to the free protons multiplicities. This point, that could be improved, in fact is not modifying the physics of fragment production.

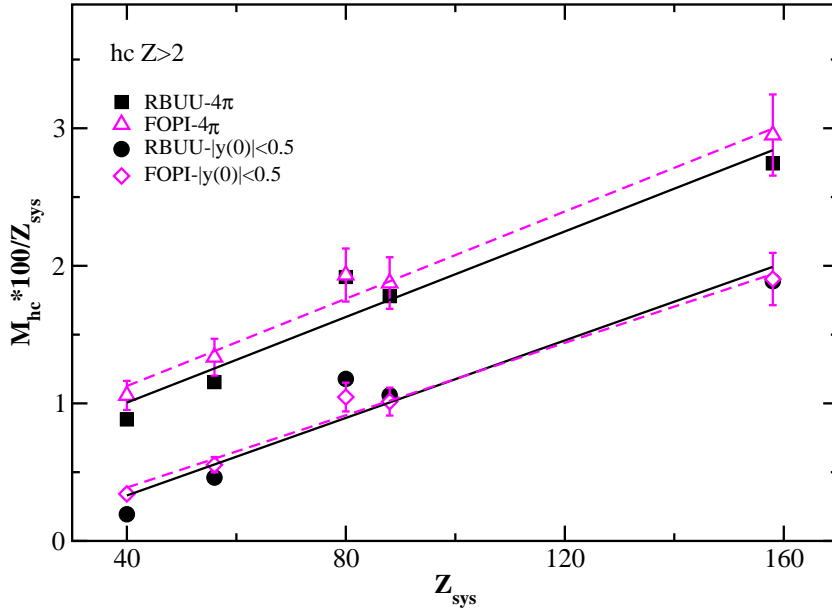


Fig. 6. Average multiplicities of heavy ($Z > 2$) clusters, normalized to those of a system with 100 protons (i.e., $M_{hc} \times 100/Z_{sys}$), as function of the system charge Z . Calculations (full symbols) and experimental data (empty) for all the phase space (4π) and confined to the midrapidity interval $|y_z^{(0)}| < 0.5$ are shown. All straight lines are linear least square fits to the symbols. The *FOPI* data are taken from Ref. [31].

The system size dependences of the fragment multiplicities, degree of stopping and maximum sideflow are summarized in Figs.6,7 and compared to the corresponding *FOPI* data.

The multiplicity of heavy clusters $Z > 2$, M_{hc} (relative to that of a 100 proton system), linearly increases with system size, independent of the phase space selections (apart the absolute values). The comparison between the theoretical calculations and the data is almost perfect, see Fig.6. In particular, the multiplicity of heavier clusters is well reproduced quantitatively, including the deviation in the system size systematics for $Z \approx 80$. This refers to the *Ru*, *Zr* systems (same mass number A , but different isospin content) and may be due to isospin effects. However, it is a very moderate effect and will not be discussed in the following. As already noted in the data, ref.[31], the good linear fits mean that the system-size dependence of M_{hc} follows a quadratic behavior vs. the system charge (mass). This further supports the two-body dominant mechanism for fragment formation.

In Fig.7 we compare to the data the size dependence of some global features of the reaction dynamics, stopping (upper panel) and maximum directed flow (lower panel). This is important to check if our transport simulations are simultaneously well reproducing attractive (radial-flows) and repulsive (side-flows)

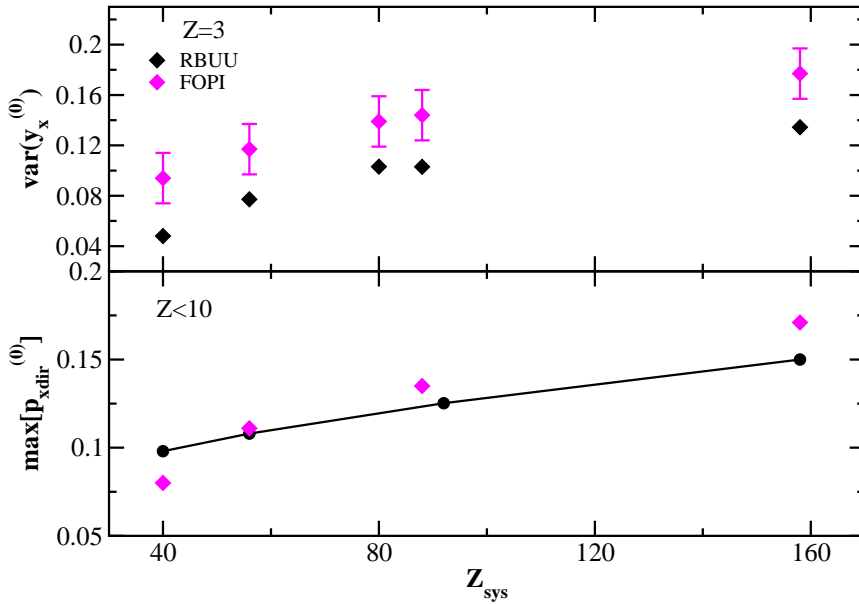


Fig. 7. Size dependences of: i) Variances of the transverse rapidity distributions for Li (upper panel), central ($b^{(0)} \leq 0.15$) collisions, data from [31]; ii) Maximal global sideflow (lower panel), semicentral collisions ($b^{(0)} \simeq 0.4$), data from [32]. The symbols have the same meaning as in the previous Fig. 6.

observables. For the stopping we report the variances in the transverse rapidity distributions of *Li* ions in central collisions. The scaled directed flow is defined as in [32], $p_{xdir}^{(0)} \equiv p_{xdir}/u_{proj}$, where $p_{xdir} = \sum \text{sign}(y) Z u_x / \Sigma Z$ (Z fragment charge, u_{proj} spatial part of the projectile 4-velocity, $u_x \equiv \beta_x \gamma$ projection of the fragment 4-velocity on the reaction plane). The sum is over all charged ions with $Z < 10$ and y the related rapidity. The maximum values reported in the simulation points of the Fig.7 (lower) correspond to the $b^{(0)} = 0.4$ scaled impact parameter [43] collision for the various systems, see [32].

The agreement is satisfying. The stopping is increasing with the system size, indicated in the enhanced values of the transverse variance with Z in Fig. 7 (upper panel). The transport estimations are systematically a little below the data since the tails of the distributions are underestimated, see the Fig. 5 bottom-right panel. This could indicate a slightly reduced radial flow. The agreement is better for the side-flow, Fig. 7 (lower panel).

This good agreement for fragment velocity distributions is not obvious, since the phenomenological parameters of the phase space coalescence model were *globally* fixed to charge distributions, without taking care of the momentum distributions. In this context it is worthwhile noting that a corresponding analysis in the framework of the Isospin Quantum-Molecular Dynamics (*IQMD*) model shows the same stopping results but cannot reproduce the fragment multiplicities with such an accuracy [31].

In general we can state that once we have fixed the physical parameters of the transport descriptions, i.e. the density dependence of the nuclear *EoS* and the in-medium NN cross sections, it turns out that the rather simple phase space coalescence model for fragment recognition works astonishingly well at intermediate incident energies. This is an important conclusion in view of the fact that most of transport models based on $(R)BUU$ – *type* approaches make use of phase space coalescence to simulate experimental selections and to reconstruct the centrality classes in the same way as in experiments, etc. [8]. We have now to better analyze the cluster formation mechanism before trying to extract some physics information on the nuclear *EoS*.

4 Clusters as probes of the nuclear *EoS*

The simulation *and* experimental results discussed in the previous section are confirming the expectations that in central *HIC* at intermediate energies fragments are originally formed in the high density phase of the reaction dynamics from fluctuations due to two-body correlations. This interpretation is mostly supported by two clear evidences: i) The correlation between fragment multiplicity and stopping, see Fig.6 and Fig.7(upper panel); ii) The linear Z_{sys} behavior of the normalized heavy cluster multiplicity of Fig.6. Such fast clusterization mechanism is completely different from the one observed at the Fermi energies, the growth of spinodal instabilities in dilute matter leading to a first order liquid-gas phase transition.

This new fragmentation dynamics opens the exciting possibility of directly probing the high density features of nuclear matter from the study of the cluster properties. However, the high density formed clusters would be largely modified during the expansion phase up to the freeze-out time. So it appears very important to follow the dynamical evolution of the clusterization in order to select the fragments that are expected to better keep the memory of the primordial high density source.

We have applied the phase space coalescence at several stages of a central $Au + Au$ collision. Fig.8 shows the mass distributions of $Z = 3, 4$ fragments at different times as indicated. It is seen that heavy clusters are identified at a very early phase of the reaction dynamics ($t \approx 10 - 30$ fm/c). In this time interval the system is in a high density phase, of around $2.5\rho_0$ and locally equilibrated, so we can speak in terms of the nuclear *EoS* [38,39]. After that time-step the system enters a fast expansion phase and the multiplicity of heavy clusters starts to decrease with a corresponding enhancement of the number of light (stable) *Li* and *Be* isotopes. We note that no sequential decay has been applied so far.

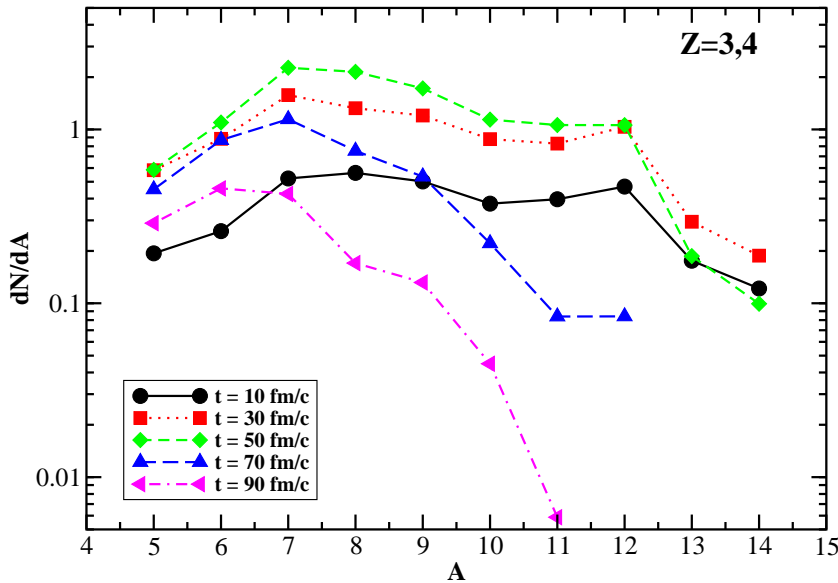


Fig. 8. Mass distributions of clusters with charges in the interval $Z = 3, 4$ at different times, as indicated, of a $Au + Au$ central collision at 0.4 AGeV incident energy.

It turns out that heavy clusters are formed very early during the high density phase whereas the evaporation of single nucleons and light fragments appear at stages after freeze-out. This picture seems not obvious since at that early stage the colliding system is still hot and highly excited. A possible answer for this surprising result could be the onset of a collective motion responsible for a fast cooling of the fireball region. In fact, in theoretical as well as in experimental studies, a strong (isotropic) radial collective flow pattern is found in intermediate energy collisions of heavy nuclei such as Au [14,48,49]. The radial flow sets in very early during the expansion phase and then rapidly governs the dynamics. Thus much of thermal energy is transferred into collective motion making the existence of heavy primary fragments possible. However, the radial flow pattern does not “freeze” the multiplicity of the early formed heavy clusters. In fact the momentum distribution of nucleons inside those clusters is still rapidly changing because of the strong radial flow component (apart the relatively small thermal and Fermi momentum components). Thus, due to the coalescence requirement in momentum space, the radial flow will imply an effective break-up of primary heavy fragments. This mechanism finally leads to the formation of light clusters.

This scenario seems to be not unrealistic: radial flow is ultimately connected with pressure gradients and thus with the achieved maximal densities. With respect to the system size the maximal density is (almost) proportional to the number of *participant* nucleons as the degree of stopping does, [32]. Similar behavior will show up in the NN collision frequency. Therefore, heavy clusters are preferentially formed in the fireball region between heavy colliding

systems relative to that of the lighter ones. As already noted, this interpretation can explain the rapidity distributions and the fragment multiplicities of the previous section (in particular the quadratic Z_{sys} dependence of Fig.6).

We conclude that the phase space coalescence model can successfully characterize the non-trivial reaction dynamics of heavy ion collisions at intermediate energies. Furthermore, the interesting evidence of an early heavy-cluster formation offers the possibility to study compressional and isospin effects at the level of fragmentation measurements. Studies based on the *IQMD* transport model [13] confirms indeed an early cluster formation and a moderate *EoS* (isoscalar) dependence of the fragment multiplicities [32]. Thus, it would be interesting to explore whether also high density isospin effects can be studied in terms of fragmentation dynamics at relativistic energies.

5 Summary and conclusions

We study in detail the mechanism of fragment production in central collisions at intermediate energies (at 0.4 AGeV). In particular we investigate the size dependence of the process in collisions of ions of different masses, where nice recent data are existing. We present a rather complete comparison of theoretical results on velocity distributions *and simultaneously* on multiplicities of all the produced particles.

Using a stochastic transport model we show the evidence of a new fast clusterization mechanism, present in the early compression stage of the reaction dynamics. The formed fragments are then propagating through the expansion phase up to the freeze-out, underlying subsequent breakings mostly due to a dynamical effect of the radial flow. As a consequence the *survived* heavier fragments will represent the *relics* of the high density phase and then could be used as direct probes of such hot and dense nuclear matter.

This scenario is supported by a series of quantitative observations, in full agreement with the existing data:

- The size dependence of charge distributions at mid-rapidity: heavier clusters are more produced from heavier systems, where larger densities can be reached in the compression stage.
- The clear correlation between heavy cluster (hc , $Z > 2$) multiplicity and global stopping.
- The quadratic dependence of cluster multiplicities on masses (charges) of the colliding ions, nice indication of the link between the *seeds* of the clusterization and the two-body correlations.

An important support to this interpretation is the possibility of a simultaneous reproduction of other global observables of the fragment dynamics, like the directed flows. The fragment recognition in all these transport simulations has been based on the very simple phase-space coalescence algorithm. Such approach appears rather reliable and this is important in view of further comparisons with experimental data, in particular for the choice of the same event selections. In fact we have also seen some limits, i.e. in the evaluation of deuteron vs. proton yields, but this point could be properly improved, see [28].

The conclusion is that observables related to fragment production in central collisions at intermediate energies can provide new independent information on the nuclear *EoS* at supra-normal densities. In particular the measurement of the isospin content of the heavier fragments appears very interesting. In the *Au + Au* case the presence of a *Isospin Distillation*, i.e. more protons bound in the clusters, would be a nice indication of a *stiff* symmetry term well above saturation density, of large astrophysics interest. This could be a good motivation for fragmentation studies at *SIS* energies with radioactive beams.

References

- [1] W.Reisdorf, H.G.Ritter, *Annu.Rev.Nucl.Part.Sci.* 47 (1997) 663; N.Hermann, J.P.Wessels, T.Wienold, *Annu.Rev.Nucl.Part.Sci.* 49 (1999) 581, and references therein.
- [2] P.Danielewicz, R.Lacey, W.G.Lynch, *Science* 298 (2002) 1592.
- [3] T.Gross-Boelting, C.Fuchs, A.Faessler, *Nucl.Phys.* A648 (1999) 105.
- [4] J.Aichelin, C.M.Ko, *Phys.Rev.Lett.* 55, (1985) 2661.
- [5] C.Sturm and the KAOS collaboration, *Phys.Rev.Lett.* 86, (2001) 39; C.Fuchs, A.Faessler, E.Zabrodin, Y.-M.Zheng, *Phys.Rev.Lett.* 86, (2001) 1974; Ch. Hartnack, H.Oeschler, J.Aichelin, *Phys.Rev.Lett.* 90, (2003) 102302.
- [6] W.Reisdorf and the FOPI collaboration, *Nucl.Phys.* A612 (1997) 493.
- [7] P.Crochet and the FOPI collaboration, *Nucl.Phys.* A624 (1997) 755; F.Rami and the FOPI collaboration, *Nucl.Phys.* A646 (1999) 367.
- [8] A.Andronic and the FOPI collaboration, *Phys.Rev.* C67 (2003) 034907.
- [9] P.Chomaz, M.Colonna, J.Randrup, *Phys.Rep.* 389 (2004) 263.
- [10] J.Pochodzalla and the ALADIN collaboration, *Phys. Rev. Lett.* 75 (1995) 1040.
- [11] C.Fuchs, P.Essler, T.Gaitanos, H.H.Wolter, *Nucl.Phys.* A626 (1997) 987.
- [12] P.Danielewicz, *Nucl.Phys.* A673 (2000) 375.
- [13] Ch.Hartnack, et al., *Eur.Phys.J.* A1 (1998) 151; S.A.Bass, et al., *Prog.Part.Nucl.Phys.* 41 (1998) 225.
- [14] P.K.Sahu, A.Hombach, W.Cassing, M.Effenberger, U.Mosel, *Nucl.Phys.* A640 (1998) 493; A.Hombach, W.Cassing, S.Teis, U.Mosel, *Eur.Phys.J.* A5 (1999) 157; A.B.Larionov, W.Cassing, C.Greiner, U.Mosel, *Phys.Rev.* C62 (2000) 064611.
- [15] T.Gaitanos, C.Fuchs, H.H.Wolter, A.Faessler, *Eur.Phys.J.* A12 (2001) 421; C.Fuchs, T.Gaitanos, *Nucl.Phys.* A714 (2003) 643; T.Gaitanos, C.Fuchs, H.H.Wolter, *Nucl.Phys.* A741 (2004) 287.
- [16] A.Andronic and the FOPI collaboration, ArXiv:nucl-ex/0411024, and references therein.
- [17] W.Botermans and R.Malfliet, *Phys.Rep.* 198 (1990) 115.
- [18] B.Blaettel, V.Koch, U.Mosel, *Rep.Prog.Phys.* 56 (1993) 1.
- [19] C.M.Ko and Q.Li, *J.Phys.* G22 (1996) 217.
- [20] S.Ayik, C.Gregoire, *Nucl.Phys.* A513 (1990) 187; J.Randrup, B.Remaud, *Nucl.Phys.* A514 (1990) 339; Y.Abe, S.Ayik, P.G.Reinhard, E.Suraud, *Phys.Rep.* 275 (1996) 49.

[21] M.Colonna, M.Di Toro, A.Guarnera, V.Latora, A.Smerzi, Phys.Lett. B307 (1993) 273;
 M.Colonna, G.F.Burgio, P.Chomaz, M.Di Toro, J.Randrup, Phys.Rev. C47 (1993) 1395.
 M.Colonna, M.Di Toro, A.Guarnera, Nucl.Phys. A580 (1994) 312.

[22] M.Colonna, M.Di Toro, S.Maccarone, M.Zielinska-Pfabe', A.Guarnera, Nucl.Phys. A642 (1998) 449.

[23] M.Colonna, G.Fabbri, M.Di Toro, F.Matera, H.H.Wolter, Nucl.Phys. A742 (2004) 337, and references therein.

[24] G.F.Bertsch, S.Das Gupta, Phys.Rep. 160 (1988) 189.

[25] J.P.Bondorf, D.Idier, I.N.Mishustin, Phys.Lett. B359 (1995) 261.

[26] J.Aichelin, Phys.Rep. 202 (1991) 233.

[27] K.Zbiri, J.Aichelin, "Origin of Fragments in Multifragmentation Reactions" in Proc. of IWM2003, GANIL/LNS, pp.28-33.

[28] L.-W.Chen, C.M.Ko, B.-A.Li, Phys.Rev. C69 (2004) 054606

[29] J.I.Kapusta, Phys.Rev. C21 (1980) 1301;
 H.Sato, K.Yasaki, Phys.Lett. B98 (1981) 153.

[30] T.Gaitanos, C.Fuchs, H.H.Wolter, Nucl.Phys. A650 (1999) 97.

[31] W.Reisdorf and the FOPI collaboration, Phys.Lett. B595 (2004) 118.

[32] W.Reisdorf and the FOPI collaboration, Phys.Rev.Lett. 92 (2004) 232301.

[33] C.Gregoire et. al., Nucl.Phys. A465 (1987) 317.

[34] C.Fuchs, H.H.Wolter, Nucl.Phys. A589 (1995) 732.

[35] H.Huber, J.Aichelin, Nucl.Phys. A573 (1994) 587.

[36] J.Cugnon et al., Nucl.Instr. and Meth. B111 (1996) 215.

[37] C. Fuchs et al., Phys.Rev. C64, (2001) 024003.

[38] V.Greco et al., Phys.Lett. B562 (2003) 215.

[39] T.Gaitanos et al., Nucl.Phys. A732 (2004) 24.

[40] K. Hagiwara, et al., Phys.Rev. D66, (2002) 010001.

[41] T.Gaitanos, C.Fuchs, H.H.Wolter, *Nuclear stopping and flows in heavy ion collisions and the in-medium NN cross section*, arXiv:nucl-th/0412055.

[42] $y_{z,x}^{(0)}$ are the *reduced* (longitudinal/transverse) rapidities normalized to the Projectile ones.

[43] $b^{(0)}$ is the *reduced* impact parameter, normalized to a $b_{max} = 1.15(A_p^{1/3} + A_t^{1/3})$.

- [44] T.Odeh and the ALADIN collaboration, Phys.Rev.Let. 84 (2000) 4557.
- [45] V.Baran, M.Colonna, M.Di Toro, Nucl.Phys. A730 (2004) 329.
- [46] T.Ericsson, W.Weise, Pions and Nuclei, Claredon, Oxford (1988).
- [47] C.R.Chen, et. al., Phys.Rev. C33 (1986) 1740.
- [48] T.Gaitanos, H.H.Wolter, C.Fuchs, Phys.Lett. B478 (2000) 79.
- [49] M.Lisa and the EOS collaboration, Phys.Rev.Lett. 75 (1995) 2662.